International Journal of Advances in Engineering and Management (IJAEM)
Volume 5, Issue 4 April 2023, pp: 280-287 www.ijaem.net ISSN: 2395-5252

A New Controller for LC-Hybrid Active Power Filter for Power Quality Improvement

K. Anil Kunar[1], S. Thirumalaiah and M. Madhusudhan Reddy[3]

1. PG Student, Department of EEE, Dr. K. V. Subba Reddy Institute of Technology, Kurnool, A.P., India
2. Assistant Professor, Department of EEE, Dr. K. V. Subba Reddy Institute of Technology, Kurnool, A.P., India
3. Assistant Professor, Department of EEE, Dr. K. V. Subba Reddy Institute of Technology, Kurnool, A.P., India

Date of Submission: 28-03-2023 Date of Acceptance: 07-04-2023

ABSTRACT:
A deadbeat current controller for an LC coupling hybrid active power filter (LC-HAPF) is suggested in this thesis, and it can track with the reference compensation current with low steady-state error and quick dynamic response. Furthermore, it allows the LC-HAPF to operate at a set switching frequency with minimal output current ripples, lowering the filtering circuit's footprint. First, the single-phase equivalent circuit is used to derive the mathematical model of the deadbeat current controller for the LC-HAPF. The closed-loop control block diagram, as well as its s-domain model, is then suggested and constructed. The suggested deadbeat current controller's stability problem and parameter design are then evaluated and explained. Finally, simulation results of the deadbeat current controller are analyzed for the LC-HAPF to the conventional hysteresis band pulse-width modulation (PWM) control, the proportional-integral (PI) control, and the proportional multi-resonant (PMR) control, demonstrating its effectiveness and superior compensating performances.

I. INTRODUCTION

The Circuit Configuration of LC-HAPF Fig.1 illustrates the system configuration of a three-phase four-wire center-split LC-HAPF, where the subscript 'x' denotes phase a, b, c, n. vsx is the system voltage, vx is the load voltage, Ls is the system inductance which can be neglected because of its small value. isx, icx and iLx are the system, inverter, load current for each phase respectively. Lcx and Ccx are the coupling inductor and capacitor of the HAPF. Cdc, VdcU and VdcL are the DC capacitor, upper and lower DC capacitor voltages with VdcU = VdcL = 0.5Vdc.The midpoint of DC-link is assumed as ground reference point g.

So that the voltage source inverter (VSI) line-to-ground voltage vinvx-g equals to VSI line-to-neutral voltage vinvx-n. T1x and T2x stand for the trigger signal of the switching device. The loads are inductive nonlinear load which are composed of three single-phase diode bridge rectifiers.It can be considered as harmonics producing loads. Fig. 5.2 shows the LC-HAPF single-phase equivalent circuit, where vCcx and vLcx represent the capacitor and inductor voltages. Parameters Design of Passive Part of LC-HAPF The coupling Lcx and Ccx of the LC-HAPF are designed based on harmonic current of loading and the average fundamental reactive power consumption.

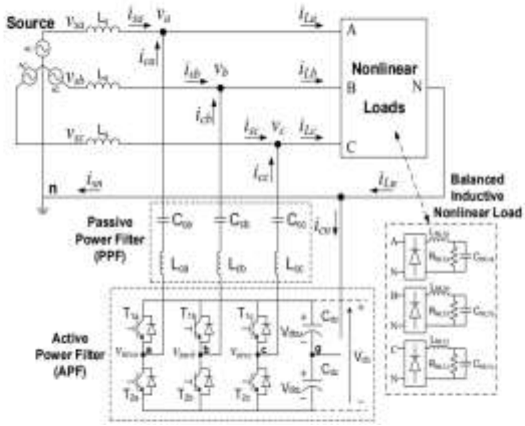

Fig. 1 System configuration of a three-phase four-wire canter-split LCHAPF.

International Journal of Advances in Engineering and Management (IJAEM)
Volume 5, Issue 4 April 2023, pp: 280-287 www.ijaem.net ISSN: 2395-5252

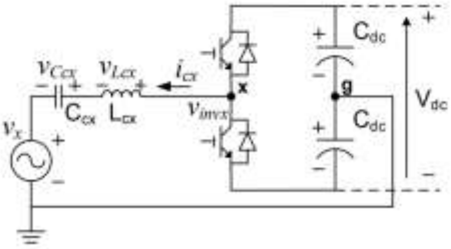

Fig. 2. LC-HAPF single-phase equivalent circuit.

Generally, the dominant harmonic orders in three-phase four-wire system are odd orders (n = 3, 5, 7…) and each LC branch can filter one single harmonic order. More LC branches can be added to the LC-HAPF to filter more harmonic current orders. Otherwise, the minimum DC-link voltage should be increased as discussed in [32]-[34].The design criteria of the Lcx and Ccx is described in the following. The relationship between the load fundamental reactive power and reactance of Lcx and Ccx can be expressed in (1), where 1 is the fundamental angular frequency, Vx represents the root-mean-square load voltage, QLxf is the load reactive power under fundamental frequency, XCcx is reactance of coupling capacitor and XLcx is reactance of coupling inductor. After that, it can solve the values of XCcx and XLcx with the help of (2). Note that n is the order of filtering harmonic frequency.In this paper, the dominant harmonic current order of the full bridge diode rectifier loading are 3rd and 5th orders, respectively. To reduce the cost and size of their coupling LC, they are tuned at the 5th order (n = 5) harmonic frequency.

II. DEADBEAT CURRENT CONTROLLER OF LC-HAPF

Proposed Deadbeat Current Controller of LC-HAPF The conventional hysteresis current PWM control for the LC-HAPF will cause significant steady-state error and also the switching frequency is variable, which implies complexity in design of the filtering circuits and the stable feedback controller for wide range operation. Thus, hysteresis PWM control usually generates large ripple and deteriorates the current harmonics compensation performance of the LC-HAPF. To overcome theseproblems, a deadbeat current controller will be proposed in this section. Fig. 3, shows a control block diagram of the proposed deadbeat current controller while Fig. 4 represents its s-domain model, in which the further analysis and discussion of the design of the controller will be presented in the following.

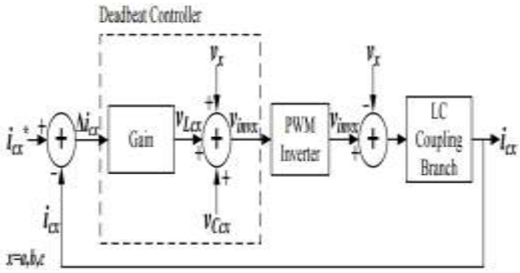

Fig. 3. Control block diagram of deadbeat current controller.

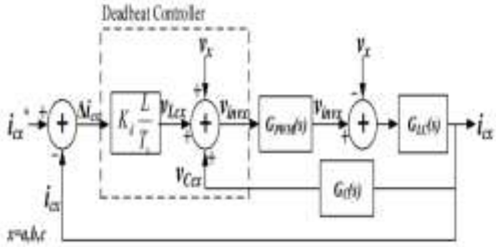

Fig. 4. s-domain model of deadbeat current controller.

Fig. 5 also shows its waveforms of generating PWM trigger signals. The key concept of this controller is to find out the duty ratio do of the switching devices in every switching period which is fixed in every single period (TSW = 1/fSW) based on the LC-HAPF system parameters, sampling period Ts and sensed instantaneous load voltage, compensation current and coupling capacitor voltage signals. After that, the trigger PWM signals for the switching devices can be generated by comparing the computed do with a triangular wave carrier with a fixed switching frequency fSW.

In addition, this deadbeat current control strategy can achieve fixed switching frequency, reduce the steady-state error, improve the performance of reference compensating current tracking and compensation performance for the LC-HAPF, which will be verified in the below section.

In the following, the mathematical modelling for the deadbeat current controller for the LC-HAPF will be introduced and discussed.

International Journal of Advances in Engineering and Management (IJAEM)
Volume 5, Issue 4 April 2023, pp: 280-287 www.ijaem.net ISSN: 2395-5252

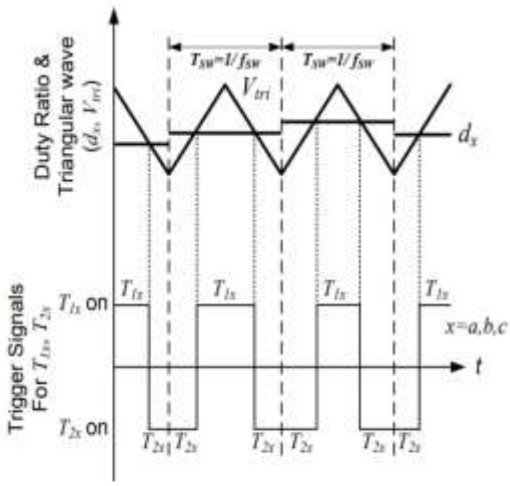

Fig. 5. Waveforms of generating PWM trigger signals with deadbeat current control.

III. MATHEMATICAL MODELLING

The reference compensating current icx * can be obtained by using the instantaneous p-q theory [46]. From Fig. 2, the characteristic equation of the LC-HAPF system can be expressed as:

$$v_{Lcx}(t) = L_{cx}\frac{di_{cx}(t)}{dt} = v_{invx}(t) - v_x(t) - v_{Ccx}(t)$$

(1)

Reforming (5.1), the averaged model of the LC-HAPF in the stationary coordinate system can be represented as:

$$v_{invx}(t) = d_x(t)\cdot v_{dc} = L_{cx}\frac{di_{cx}(t)}{dt} + v_x(t) + v_{Ccx}(t)$$

(2)

Where dx refers to the duty ratio in one phase of the VSI in each small-time interval. It can be separated by upper and lower switch part as follows:

$$d_{Ux}(t) + d_{Lx}(t) = 1$$

(3)

The summation of them is equal to 1 since the switching ON and OFF time of the upper and lower switches of the VSI is equal to one control switching period (TSW=1/fSW). From (3), the characteristic equation (1) becomes:

$$\left[d_{Ux}(t) - d_{Lx}(t)\right]\cdot v_{dc} = L_{cx}\frac{di_{cx}(t)}{dt} + v_x(t) + v_{Ccx}(t)$$

(4)

For digital implementation of the PWM control algorithm and the consideration about the filter inductance deviation, the instantaneous averaged model in (4) can be represented in discrete time with a step size of k as in (5):

$$\left[d_{Ux}(k) - d_{Lx}(k)\right]\cdot v_{dc} = K_d L_{cx}\frac{i_{cx}(k+1) - i_{cx}(k)}{T_s} + v_x(k) + v_{Ccx}(k)$$

(5)

Where Kd is inductance deviation coefficient that can be treated as control variable, Ts is the sampling period. icx(k+1) represents the reference compensating current icx *.Hence, combining (3) and (5), the duty ratio of one phase VSI is now obtained as:

$$\left.\begin{array}{l} d_{Ux}(k) = \dfrac{1}{2}\left[1 + \dfrac{K_d L_{cx}\dfrac{i^*_{cx}(k) - i_{cx}(k)}{T_s} + v_x(k) + v_{Ccx}(k)}{v_{dc}}\right] \\ d_{Lx}(k) = \dfrac{1}{2}\left[1 - \dfrac{K_d L_{cx}\dfrac{i^*_{cx}(k) - i_{cx}(k)}{T_s} + v_x(k) + v_{Ccx}(k)}{v_{dc}}\right] \end{array}\right\}$$

(5.6)

Usually, find out the duty ratio of either upper or lower switch (dUx (k) or dLx (k)) is enough, then find out the duty ratio of the remaining switch by using (3). After that, the duty ratio is used to compare with the fixed frequency triangular carrier wave in order to generate PWM signal for the switching devices in VSI. The switching frequency of the VSI is the same as the frequency of the triangular carrier wave. Stability and Parameter Design of Deadbeat Current Controller According to (7) and Fig.3, Fig.4 shows the s-domain closed-loop control block diagram model for the deadbeat current controller of the LC-HAPF. The information of each block will be given in below. GPWM(s) is an average s-domain model, note that the PWM VSI can be assumed as unity gain [44], in which Fig.6 shows the details of GPWM(s). To accurately describe the GPWM(s), computation delay, sampler and zero order hold (ZOH) as in s-domain should be considered. The transfer function of the PWM VSI can be expressed as:

$$G_{PWM}(s) = \frac{e^{-T_s \cdot s}\left(1 - e^{-T_s \cdot s}\right)}{T_s \cdot s}$$

(7)

Where Ts is the sampling time.For obtaining a rational transfer function, delays are usually approximated by poles and then, Pade' approximation (8) can be applied to (7).

International Journal of Advances in Engineering and Management (IJAEM)
Volume 5, Issue 4 April 2023, pp: 280-287 www.ijaem.net ISSN: 2395-5252

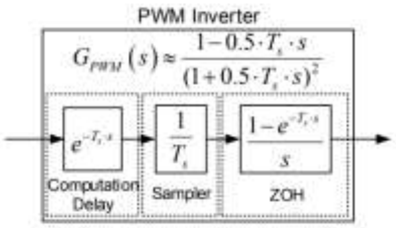

Fig. 5.6. s-domain model of PWM inverter zeros.

$$e^{-T_s \cdot s} \approx \frac{1-0.5 \cdot T_s \cdot s}{1+0.5 \cdot T_s \cdot s}$$

(8)

Substitute (8) into (7) yields:

$$G_{PWM}(s) = \frac{e^{-T_s \cdot s}(1-e^{-T_s \cdot s})}{T_s \cdot s} \approx \frac{1-0.5 \cdot T_s \cdot s}{(1+0.5 \cdot T_s \cdot s)^2}$$

(9)

Where GLC(s) and GC(s) are the LC coupling branch and coupling capacitor impedance in s-domain, which can be expressed as follows:

$$G_{LC}(s) = \frac{C_{cx}s}{L_{cx}C_{cx}s^2+1}$$

$$G_C(s) = \frac{1}{C_{cx}s}$$

(10)

The transfer function according to Fig. 4 can be deduced as:

$$i_{cx}(s) = G_{CL\_i}(s) \cdot i_{cx}^*(s) + G_{CL\_v}(s) \cdot v_x(s)$$

$$= \frac{K_d \frac{L}{T_S} G_{PWM}(s) G_{LC}(s)}{1+K_d \frac{L}{T_S} G_{PWM}(s) G_{LC}(s) - G_{PWM}(s) G_{LC}(s) G_C(s)} i_{cx}^*(s) + \frac{G_{LC}(s)(G_{PWM}(s)-1)}{1+K_d \frac{L}{T_S} G_{PWM}(s) G_{LC}(s) - G_{PWM}(s) G_{LC}(s) G_C(s)} v_x(s)$$

(11)

Where GCL_i(s) is the system closed-loop transfer function between icx and icx* ,GCL_v(s) is the system closed-loop transfer function between icx and vx. To analyse the stability of the proposed deadbeat current controller, the range of the control coefficient Kd must be found. Theoretically, Kd should be as high as possible to obtain high gain, fast response and low steady-state error at low-order harmonics frequency and fundamental frequency.

However, system stability is under the 1st priority consideration. The stability margin would be sacrificed with high Kd gain. Therefore, with the help of the Routh's stability criterion and Fig. 4, the analysis of the range of Kd is based on the characteristic equation (q(s) = 0) of the closed-loop transfer function between icx and icx *.The closed-loop transfer function between icx and icx * is shown in (12) and its characteristic equation can be expressed in (13).

$$G_{CL\_i}(s) = \frac{K_d \frac{L}{T_S} G_{PWM}(s) G_{LC}(s)}{1+K_d \frac{L}{T_S} G_{PWM}(s) G_{LC}(s) - G_{PWM}(s) G_{LC}(s) G_C(s)}$$

(12)

$$q(s) = 1+K_d \frac{L}{T_S} G_{PWM}(s) G_{LC}(s) - G_{PWM}(s) G_{LC}(s) G_C(s) = 0$$

(13)

According to the stability criterion, the first column of Routh's array needs to be larger than 0 in order to guarantee the system stability. After mathematical calculation, the range of Kd can be obtained as:

$$0 < K_d < \frac{4}{3} + \frac{1}{6} \frac{T_S^2}{L_{cx}C_{cx}}$$

(14)

TS (Since the term 1/6 2 /LcxCcx is very small, it can be neglected for simplicity.Hence, the range of Kd can be obtained as:

$$0 < K_d < \frac{4}{3}$$

(15)

The deduced model of the deadbeat current control loop of the LC-HAPF is analyzed by using MATLAB and the system parameters including different Kd range is given in Table I.

As mentioned before, Kd should be selected as high as possible within the bounded value to minimize the steady-state error and shorten the response time. However, high Kd value will cause overshoot problem and lower the stability margin.

Table I

SYSTEM PARAMETERS FOR MATLAB SIMULATION

System parameters	Physical values
L_{cx}, C_{cx}	8mH, 50μF
f_0 (fundamental frequency)	50 Hz
f_S (sampling frequency)	15 kHz
f_{sw} (switching frequency: deadbeat control)	10 kHz
K_d	0.2~1.2

To obtain a balance on steadystate error, overshoot and response time, Kd should be selected in around 0.8 to 1.1, which depends on desired performance. In this paper, Kd = 0.8 is chosen. The deduced model of the deadbeat current control loop of the LC-HAPF is analyzed by using MATLAB

International Journal of Advances in Engineering and Management (IJAEM)
Volume 5, Issue 4 April 2023, pp: 280-287 www.ijaem.net ISSN: 2395-5252

and the system parameters including different Kd range is given in Table II.As mentioned before, Kd should be selected as high as possible within the bounded value to minimize the steady-state error and shorten the response time. However, high Kd value will cause overshoot problem and lower the stability margin. That means icx˜ icx* , the compensating current can track its reference with less steady-state error, thus obtaining better current tracking performance. To obtain a balance on SteadyState error, overshoot and response time, Kd should be selected in around 0.8 to 1.1, which depends on desired performance.

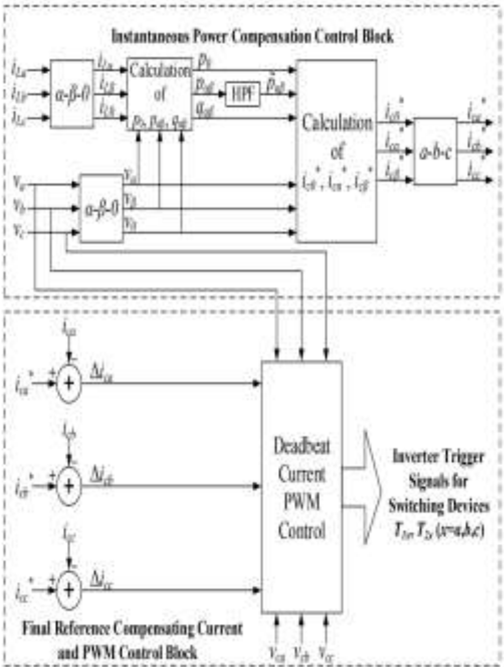

Fig. 8. The block diagram of proposed deadbeat current controller.

IV. SIMULATION RESULTS

In the following, the simulation studies of the conventional hysteresis PWM controller, PI controller, MPR controller and deadbeat current controller for the three-phase four-wire center split LC-HAPF are carried out by using PSCAD/EMTDC.The corresponding simulation results before and after the hysteresis PWM controlled, the PI controlled, the MPR controlled and the deadbeat current controlled LC-HAPF compensation will be summarized in Fig. 9.

With reference to the IEEE standard 519-2014 [47], the acceptable Total Demand Distortion (TDD) = 15% with ISC/IL is in 100 < 1000 scale (a small rating 110V-5kVA experimental prototype). The nominal rate current is assumed to be equal to the fundamental load current at the worst-case analysis, which results in THD = TDD =15%.Therefore, this paper evaluates the LC-HAPF current harmonics compensating performance by setting an acceptable THD =15%.

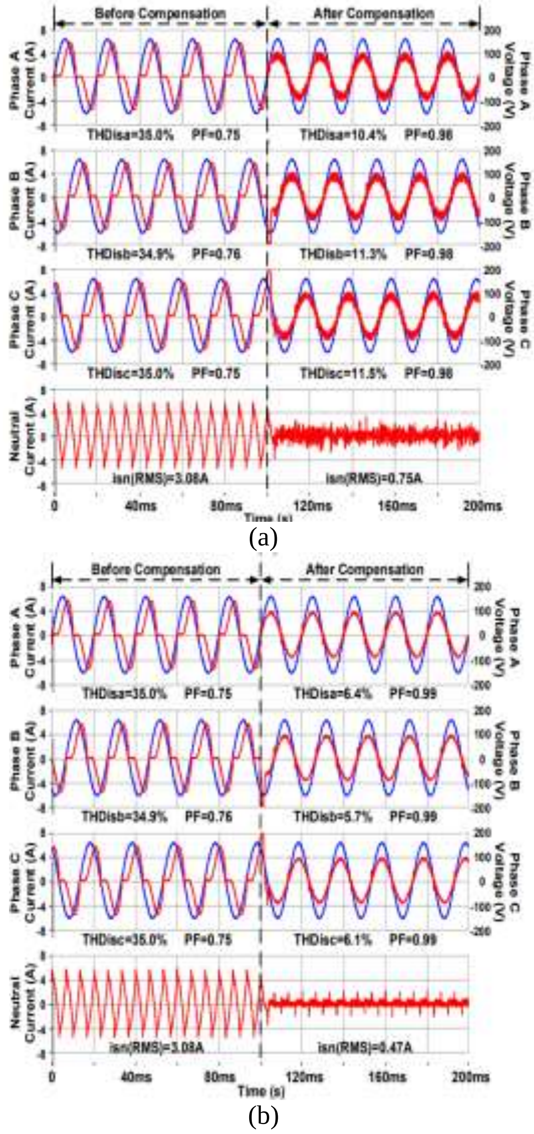

Fig. 5.9 (a). Simulated results before and after LC-HAPF compensation with PI controller and (b) with proposed Dead-beat controller

The basic control principle of the hysteresis PWM control is based on deriving the switching signals from the comparison of the current error ?icx between the reference compensating current icx * and the actual compensating current icx with a fixed hysteresis band H.The trigger signals will drive the switching devices of the VSI in order to let icx tracks with its reference icx* . Every time when the current error ?icx is larger than the positive or smaller than the negative hysteresis band's boundary icx *+H or

International Journal of Advances in Engineering and Management (IJAEM)
Volume 5, Issue 4 April 2023, pp: 280-287 www.ijaem.net ISSN: 2395-5252

icx* -H, a state change of the VSI's trigger signals occurs.The PI and PMR control is initially computing the current error signalicx by subtracting the reference compensating current icx * by the actual compensating current icx, ?icx will be inputted into a PI / PMR controller. Then its corresponding output will be compared with a fixed frequency triangular carrier wave Vtriin order to generate the trigger signals for the switching devices of the VSI. Hysteresis PWM Controller Fig. 9(a) shows the simulation results of hysteresis PWM controller for the LC-HAPF. From Fig. 9(a), the system current ripples after compensation is obvious. From Fig. 9(a) and Table IV, although it can compensate the system displacement power factor (DPF) from 0.8 to unity, the system neutral current from 3.08Arms to 0.75Arms, the total current harmonics distortion (THDisx) from 35% to about 11%, which satisfies the international standard of THD =15% [47]. The system current ripples have been reduced significantly compared with the hysteresis PWM controller after compensation.

Deadbeat Current Controller Fig. 9(b) shows the simulation results of deadbeat current controller for the LC-HAPF. Compared with hysteresis PWM controller case, the system current ripples after compensation have been reduced significantly. From Fig. 9(b), it can compensate the system DPF from 0.8 to unity, the system neutral current from 3.08Arms to 0.47Arms, the THD isx from 35% to less than 6.5%, which satisfies the international standard of THD =15% [47]. It has the lowest percentage error of reactive power injection of less than 1%.

V. CONCLUSION

In this paper, an LCHAPF deadbeat current control approach is suggested, which may offer a cost-effective power quality compensation solution with minimal output current ripples and modest steady-state error. First, the suggested deadbeat current controlled LC-mathematical HAPF's modelling, and control block diagram are created and constructed. It is used to assess and debate the stability problem as well as parameter design considerations. Finally, the results of the deadbeat current controller for the LC-HAPF are shown in contrast to traditional hysteresis, PI, and PMR controllers, demonstrating its efficacy and improved compensatory capabilities.

REFERENCES

[1]. W. G. Morsi and M. E. El-Hawary, "Defining Power Components in Nonsinusoidal Unbalanced Polyphase Systems: The Issues," IEEE Trans. Power Deliv., vol. 22, no. 4, pp. 2428–2438, 2007.

[2]. H. Fujita and H. Akagi, "A practical approach to harmonic compensation in power systems-series connection of passive and active filters," IEEE Trans. Ind. Appl., vol. 27, no. 6, pp. 1020–1025, 1991.

[3]. L.H.S. Duarte & M.F. Alves, "The degradation of power capacitors under the influence of harmonics", Proc. IEEE 10th Int. Conf. on Harmonics and Quality of Power, vol. 1, pp. 334–339, 2002.

[4]. J. S. Subjak, Jr. and J. S. McQuilkin, "Harmonics-Causes, effects, measurements, and analysis: An Update," IEEE Trans. Ind. Appl., vol. 26, no. 6, pp. 1034-1042, 1990.

[5]. R.C. Dugan, M.F. McGranaghan, H.W. Beaty, Electrical power systems quality. New York: McGraw-Hill, pp. 36, 1996.

[6]. J.C. Das, "Passive filters - potentialities and limitations," IEEE Trans. Ind. Appl., vol.40, no.1, pp.232-241, Feb. 2004.

[7]. S. T. Senini and P. J. Wolfs, "Systematic identification and review of hybrid active filter topologies," in Proc. IEEE 33rd Annu. Power Electron. Spec. Conf., vol. 1, pp. 394–399, 2002.

[8]. F. Z. Peng, H. Akagi, and A. Nabae, "A new approach to harmonic compensation in power systems: A combined system of shunt passive and series active filters," IEEE Trans. Ind. Appl., vol. 26, no. 6, pp. 983–990, Nov./Dec. 1990.

[9]. H. Hu, Y. Xing, "Design considerations and fully digital implementation of 400-Hz active power filter for aircraft applications," IEEE Trans. Ind. Electron., vol.61, no.8, pp.3823-3834, Aug. 2014.

[10]. A. B. Plunkett, "A current-controlled PWM transistor inverter drive," Conf. Rec. 14th Annu. Meet. IEEE Ind. Appl. Soc., pp. 785-792, 1979

[11]. L. Malesani and P. Tenti, "A novel hysteresis control method for current-controlled voltage-source PWM inverters with constant modulation frequency" IEEE Trans. Ind. Appl., vol. 26, no. 1, pp. 88-92, 1990.

[12]. A. Fereidouni, M. A. S. Masoum, K. M. Smedley, "Supervisory Nearly Constant Frequency Hysteresis Current Control for Active Power Filter Applications in Stationary Reference Frame," IEEE Power

and Energy Technology Systems Journal, vol. 3, pp. 1-12, 2016.
[13]. N. M. Ismail and M. K. Mishra, "Study on the design and switching dynamics of hysteresis current controlled four-leg voltage source inverter for load compensation," IET Power Electron., vol. 11, no. 2, pp. 310-319, 2018.
[14]. M. P. Kazmierkowski, R. Krishnan, and F. Blaabjerg, "Control in power electronics: selected problems," Amsterdam: Academic Press, 2003.
[15]. A. Chandra, B. Singh, B.N. Singh and K. Al-Haddad, "An improved control algorithm of shunt active filter for voltage regulation, harmonic elimination,power-factor correction, and balancing of nonlinear loads," IEEE Trans. Power Electron., vol.15, no.3, pp. 495-507, 2000.
[16]. P. Jintakosonwit, H. Fujita, and H. Akagi, "Control and performance of a fully-digital-controlled shunt active filter for installation on a power distribution system," IEEE Trans. Power Electron., vol. 17, no. 1, pp. 132–140, Jan. 2002.
[17]. S. Rahmani, N. Mendalek and K. Al-Haddad, "Experimental design of a nonlinear control technique for three-phase shunt active power filter," IEEE Trans. Ind. Electron., vol. 57, no. 10, pp. 3364 - 3375, 2010.
[18]. R. Teodorescu, F. Blaabjerg, M. Liserre, and P. C. Loh, "Proportionalresonant controllers and filters for grid-connected voltage-source converters," IEE Proceedings - Electric Power Applications, vol. 153, no. 5, pp. 750–762, 2006.
[19]. M. Liserre, R. Teodorescu and F. Blaabjerg, "Multiple harmonics control for three-phase grid converter systems with the use of PIRES current controller in a rotating frame," IEEE Trans. Power Electron., vol.21, no.3, pp.836-841, 2006.
[20]. T. Hornik and Z. Qing-Chang, "A current-control strategy for voltage source inverters in microgrids based on h8 and repetitive control," IEEE Trans. Power Electron, vol. 26, pp. 943-952, 2011.
[21]. L. Herman, I. Papic, and B. Blazic, "A proportional-resonant current controller for selective harmonic compensation in a hybrid active power filter," IEEE Trans. on Power Deliv., vol. 29, no. 5, pp. 2055-2065, 2014.
[22]. A. Javadi, L. Woodward, and K. Al-Haddad, ‘‘Real-time implementation of a three-phase THSeAF based on a VSC and a P+R controller to improve the power quality of weak distribution systems,’’ IEEE Trans. Power Electron., vol. 33, no. 3, pp. 2073–2082, Mar. 2018.
[23]. N. Xie, Q, Xu, J, Zeng, X, Liu, W. Zhang and C. Zhang, "Noval hybrid control method for APF based on PI and FRC", IET The Journal of Engineering, vol. 2019, no. 16, pp. 3002-3006, 2019.
[24]. D. G. Holmes and D. A. Martin, "Implementation of direct digital predictive current controller for single and three phase voltage source inverters," Conf. Rec. IEEE-IAS Annu. Meeting, pp. 906–913, 1996.
[25]. S. Buso, L. Maleasani, and P. Mattavelli, "Comparison of current control techniques for active power filter applications', IEEE Trans. Ind. Electron., vol. 45, no. 5, pp. 722-729, Oct. 1998.
[26]. K. Nishida, T. Ahmed and N. Nakaoka, "Robust deadbeat current control with adaptive predictor for three-phase voltage-source active power filter", Proc. of 39th Annual Industry Application Conference, Oct. 2004.
[27]. M. Odavic, V. Zanchetta, P. Sumner, and M. M. Degano, "One-sample- period-ahead predictive current control for high-performance active shunt power filters," IET Power Electron., vol. 4, no. 4, pp. 414–423, Apr. 2011.
[28]. B.-J. Kim, S.-C. Choi, S.-H. Bae, and C.-Y. Won, "An improved deadbeat control method based on current predictive algorithm for shunt active power filter," 2015 IEEE 2nd International Future Energy Electronics Conference (IFEEC), 2015.
[29]. W. Jiang, X. Ding, Y. Ni, J. Wang, L. Wang, and W. Ma, "An improved deadbeat control for a three-phase three-line active power filter with current-tracking error compensation," IEEE Trans. Power Electron., vol. 33, no. 3, pp. 2061–2072, 2018.
[30]. S. Srianthumrong and H. Akagi, "A medium-voltage transformerless ac/dc power conversion system consisting of a diode rectifier and a shunt hybrid filter," IEEE Trans. Ind. Appl., vol. 39, no. 3, pp. 874-882, 2003.

[31]. C.-S. Lam, M.-C. Wong and Y.-D. Han, "Hysteresis current control of hybrid active power filters," IET Power Electron., vol.5, no. 7, pp. 1175-1187, Aug. 2012.
[32]. C.-S. Lam, X.-X. Cui, W.-H Choi, M.-C. Wong and Y.-D. Han, "Minimum inverter capacity design for three-phase four-wire LC-hybrid active power filters," IET Power Electron. vol. 5, no. 7, pp. 956-968, Aug. 2012.
[33]. C.-S. Lam, W.-H. Choi, M.-C. Wong, and Y.-D. Han, "Adaptive dc-link voltage controlled hybrid active power filters for reactive power